Influence of crystal material on the performance of the HiRez 3D PET scanner: A Monte-Carlo study

C. Michel, L. Eriksson, H. Rothfuss, B. Bendriem

Siemens Medical Solutions, Molecular Imaging, Knoxville, TN, 37932, USA

D. Lazaro, *CEA LIST Saclay, France*,

I. Buvat, *U678 Inserm, CHU Pitié Salpêtriere, Paris, France*

***Abstract*— The quest for the ideal inorganic scintillator is still active in PET. The aim of this investigation is to study the imaging performance of a 3D PET system as a function of the crystal when considering the HiRez scanner geometry and its Pico acquisition system. A realistic Monte-Carlo model of the scanner was developed using GATE. The model was tuned to measurements using the NEMA NU2-2001 protocol. Measured energy resolution, time window and energy window were inputs in the simulation, while measured front-end deadtime was introduced externally. Small discrepancies between experiment and simulation were described by relative efficiencies for singles and coincidences. The model was modified by replacing LSO by BGO, GSO, $LaBr_3$ and $CeBr_3$, for two different crystal lengths (20 and 30mm). Energy resolution, energy window, time coincidence window and deadtime parameters were adapted in each case. NEC curves were obtained by scaling the experimental HiRez sensitivity for singles and coincidences to the GATE results. The result shows that only the LSO 30 mm case provides superior NEC performance when the axial scanner length is fixed. Considering the HiRez geometry, LSO appears to yield the best imaging performance as measured by peak NEC, due to the combination of high speed and high stopping power.**

I. INTRODUCTION

The quest for the ideal organic scintillator in PET is still very active. Although BGO remains a very attractive material due to its high density and excellent stopping power, its performance is poor in the activity range required by whole-body PET. Currently, it is replaced by LSO, LYSO, GSO, $LaBr_3$ or $CeBr_3$ due to their faster timing. This substitution allows a reduction in random rate, system deadtime and has the potential to improve SNR by using Time-Of-Flight (TOF). The present work investigates via Monte-Carlo simulation the potential gain of substituting another scintillator in the current HiRez with its Pico electronics. It extends our previous work on the ECAT EXACT geometry [1]. The model is first validated with experimental HiRez data [2] and later used in a predictive way with other scintillators, varying crystal length. A similar study was published on pixelated Anger-logic detectors (Gemini, commercialized by Philips) [3]. On that system it was found that $LaBr_3$ (30mm) outperforms LSO (20mm) above 0.35 μCi/cc. The question addressed in this study is whether we get a similar answer on the HiRez system or whether this result was specific to that scanner design.

II. METHODS

A. HiRez modeling

A Monte-Carlo model of the current HiRez PET scanner including 3 rings of 48 LSO blocks (13 x 13 matrix of 4mm x 4 mm x 20 mm crystals) was developed using GATE [4]. New classes were introduced in GATE to handle the spherical geometry of the scanner. A spherical repeater was developed to position the blocks along a sphere, given five parameters: the sphere radius, the numbers of blocks in the axial direction and in the transaxial direction, and the angle value between two blocks in the axial direction and in the transaxial direction. Care was taken in the simulation to include a precise description of all materials included in the scanner: bed, external shields, tunnel, block detector casing. The scintillation light transport and its detection were not modeled explicitly but accounted for during analysis with a global energy resolution parameter also assuming proportionality between energy deposition and scintillation light production. Variations of energy resolution inside the block were also neglected. Crystal identification used the center of the crystal where the maximum energy deposition occurred. In the analysis, the crystal position was blurred axially and transaxially to account for the Anger positioning logic. The amount of blurring (3.5 mm) was adjusted to match the measured spatial resolution (data not shown). Singles events above constant fraction discriminator (CFD) threshold and energy qualified singles (inside the energy window LLD-ULD) were recorded in ROOT format [5]. Prompt (P) coincidences between energy qualified singles were also recorded in ROOT and subsequently sorted in sinogram format as either True unscattered (T), True scattered (S) and Random (R), accounting for axial compression (span and maximum ring difference). The GATE digitizer was set to record only one event per multiple. With GATE, random and scatter inside the prompt coincidence window are known exactly so that P = T+S+R. We did not simulate a delayed coincidence window, since we were not interested in reproducing the performance at very high count rate (i.e. the saturation of the total coincidences (P+R) count rate). Sinogram data were scored in the 24 cm FOV, as prescribed by the NEMA NU2-2001 specifications. The LSO background was added in the singles in the deadtime model external to GATE. No LSO coincidence

1-4244-0561-0/06/$20.00 ©2006 IEEE.

background was added to the coincidences due to the high selected LLD. Equations 1-5 [1] were used to describe the NEMA NU2-2001 NEC experimental data for the HiRez [2]:

$$S_{dtc} = \eta_{si} * \alpha + bkg_{LSO} \quad (1)$$

$$S_{obs} = S_{dtc} * e^{-c_1 * \tau * S_{dtc}} \quad (2)$$

$$\mathrm{T+S} = \eta_{tr} * \alpha * \left[e^{-c_2 * \tau * S_{dtc}}\right]^2 \quad (3)$$

$$\mathrm{R} = {S_{dtc}}^2 * \Delta\tau * n_{lor} * \left[e^{-c_3 * \tau * S_{dtc}}\right]^2 \quad (4)$$

$$NEC_{1R} = \frac{T^2}{P} \quad (5)$$

In these equations, S_{obs} and S_{dtc} are the observed and deadtime corrected singles rates; τ is integration and reset time given by $\tau = n_{integration} * \tau_{scint} + t_{reset}$, where τ_{scint} is the crystal scintillation time and t_{reset} is fixed at 10 ns; bkg_{LSO} is the ^{176}Lu background, η_{si} and η_{tr} are the single and true (unscattered + scattered) coincidence sensitivity in c/s/μCi/cc, α is the activity average concentration in the phantom, $\Delta\tau$ is the coincidence time window, c_1 is the ratio between singles above CFD threshold (50 keV) and singles in the qualifying energy window (425 - 650 keV); c_2 and c_3 are similar to c_1 but account for additional deadtime when multiplexing singles from 6 blocks and n_{lor} is the amount of possible LOR's passing through the 20 cm diameter phantom. Since the energy distribution and incidence angle for the singles impinging on the detectors differ for true and random coincidences, c_2 and c_3 are expected to be slightly different. NEC_{1R} assumes the variance on T is P (and not P+R). This requires that either a variance reduction is applied on delayed coincidences or that randoms are estimated from singles. When fitting these equations to the GATE predictions, we estimated f_{si} as the ratio between measured and predicted singles sensitivity, f_{tr} as the ratio between measured and predicted sensitivities for the true (T+S) coincidences and f_{ra}, as the ratio between measured and predicted sensitivities for the random coincidences.

B. Modeling of other materials and crystal lengths

The GATE model was modified by replacing LSO by GSO, BGO, $LaBr_3$ and $CeBr_3$, for two different crystal lengths (20 and 30 mm). LYSO was not considered, since the results were expected to be very similar to the LSO case. For LSO 30mm, the LSO singles background was scaled from the HiRez value according to the LSO volume. In each case, energy resolution, energy window and time coincidence window were adapted to realistic values. Integration time was set proportional to the crystal decay time times a multiplicative factor varying from 3 for LSO and GSO, 2 for LaBr3 and CeBr3 and 1.3 for BGO.

The estimated NEC_{1R} curves were obtained by scaling the experimental HiRez sensitivity (LSO 20 mm) for singles and coincidences to the GATE simulation results obtained at one single activity level (0.053 Ci/cc) for all material and length crystal combinations and by adjusting deadtime parameters to appropriate values: c_1 was directly provided by GATE while the ratio c_2/c_1 and c_3/c_1 were identical to HiRez experimental values. This procedure ensures that additional multiplexing deadtime for true and random coincidences in the Pico electronics is identical in all cases.

III. RESULTS

A. HiRez (LSO 20 mm)

For the NEMA NU2-2001 NEC measurement, the scatter fraction (34.7%) matches the GATE prediction (35.5%). The measured energy qualified singles are described by eq. (1-2) using η_{si}=341750, c_1=3.42, and bkg_{LSO}=5670c/s, with τ fixed at 136 ns. Experimental trues corrected for scatter (T) are described by eq. 3 (when S=0) with $\eta_{tr\_unscattered}$=572091, c_2=6.57 while randoms require c_3=5.73 with $\Delta\tau$ fixed at 4.5 ns.

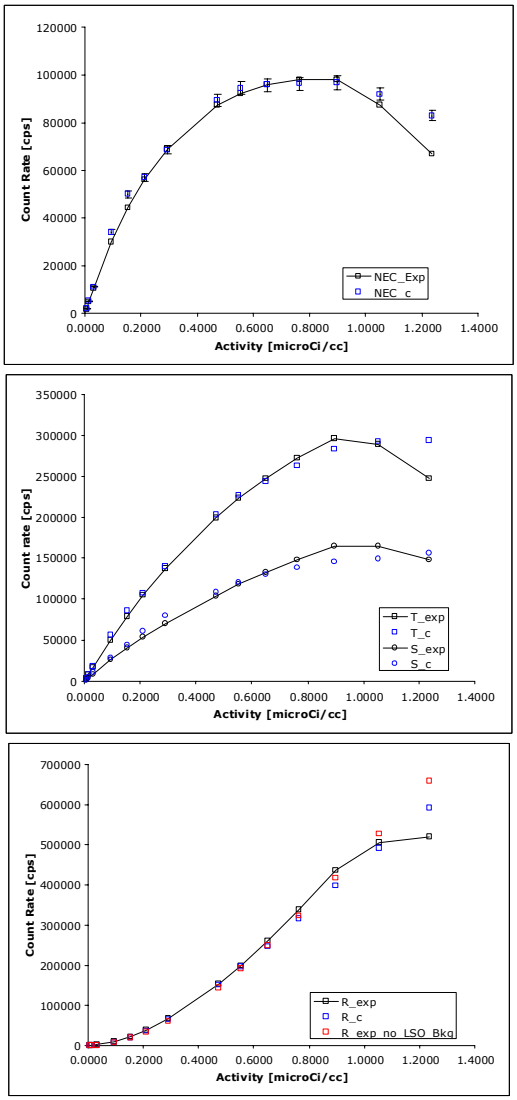

Fig 1: Comparison between measured and predicted NEC_{1R} curves (top), True and Scatter (center), and Random (bottom). The experimental data are solid black curves. The GATE predictions (after rescaling) are shown in blue.

The GATE predictions for singles, true and random coincidences were rescaled by f_{si}=82%, f_{tr}=94% and f_{ra}=84% to match with experimental data, respectively. These results are illustrated in Figure 1, showing the NEC_{1R}, True (T+S) and

Random experimental data compared to rescaled GATE predictions. The value of c_1 provided by GATE is 3.33.

B. Modeling of other materials and crystal lengths

Table 1 provides the value of the parameters used in equations (1-5) to calculate the NEC_{1R} curves for all material and crystal length combinations. The GATE predictions for the scatter fractions are also provided. The GATE predictions at the lowest activity for both singles and true coincidences sensitivities were normalized to the experimental HiRez values. The normalization factors are reported as η_{si_rel} and η_{tr_rel} in the table. Figure 2 displays the NEC curves estimated with these parameters.

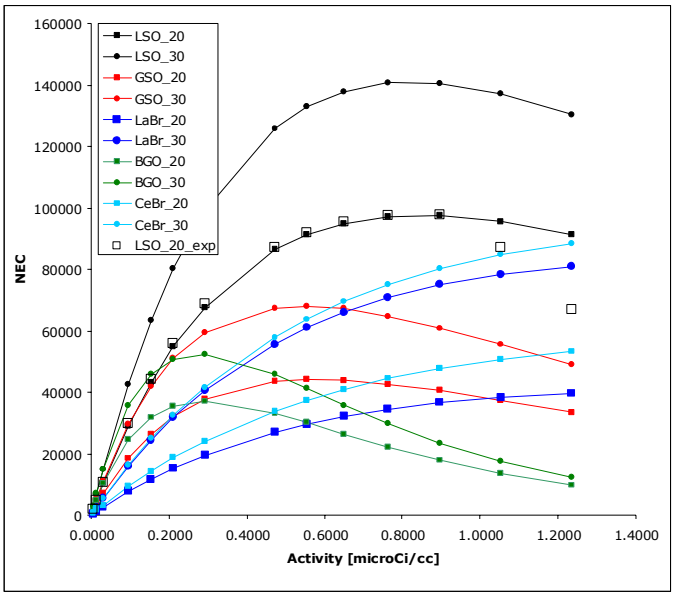

Fig 2: NEC_{1R} curves for all material-crystal length combinations

IV. Discussion

This study was undertaken to examine if LSO was the best detector material to use in the HiRez wholebody scanner given its geometry and the Pico electronics, since it was shown that smaller stopping power could be compensated in NEC performance by smaller deadtime (shorter decay time) and smaller scatter fraction (better energy resolution) [3]. We analyzed the experimental NEC data for the HiRez [2] with a customized NEC model including the relevant deadtime parameters (block detector and multiplexing) and accounting for LSO background [1]. The same model was applied to the GATE simulated data rather than modeling the processing chain (digitizer) inside GATE. The singles and coincidence background from ^{176}Lu decay were not simulated inside GATE but accounted for externally since the energy of qualified singles (LLD = 425 keV) was above the 307 keV transition in ^{176}Hf, which minimized the rate of additional coincidences. However, LSO background simulation within GATE should be preferred when simulating very weak sources with lower discriminator values [6]. Our procedure is simple and could be the preliminary step before deadtime modeling within GATE by adjusting successively the deadtime parameters for singles, random and true coincidences. Our approach is valid as long as we are interested in global NEC performance and not in reconstructing noisy images from simulated data. We recorded singles both above CFD threshold and in the LLD-ULD window just to validate c_1. Our model did not try to reproduce the saturation in total number of coincidences (P+R), experimentally observed around 1 Ci/cc, therefore random coincidences were not generated in a separate delayed window, but were identified in the prompt coincidences by using GATE event identifiers associated with each detected gamma-ray. Ideally, two scaling factors (one for singles and one for coincidences) should suffice to explain the discrepancy between simulated and experimental data. In our case, three independent rescaling factors (for singles, trues and randoms) were found necessary for superimposing HiRez experimental data to GATE simulation. These three factors are likely due to (i) residual discrepancies between the true scanner geometry and its limited description inside GATE and (ii) over-simplification of the data processing chain (e.g. same energy resolution for all crystals within the block, same CFD threshold for all blocks). One should also note that some dispersion exists in the HiRez measured NEC curves which could be attributed to e.g. differences in activity calibration and/or scanner set-up and would require either smaller or larger scaling factors (see e.g. [7]).

When modeling other materials and estimating their NEC curves we used a common deadtime model and realistic parameters (Table 1), exploiting the differences in scintillation times and achievable energy resolution on small crystals. The minimum value of the coincidence window was 4.5 ns, which corresponds to the TOF difference between the two gamma-rays on the 67.5 cm FOV (i.e. a smaller coincidence window would decrease the sensitivity at the FOV border).We also normalized singles, true and random coincidences to the HiRez experimental data. This procedure was convenient since it required only one single simulation per case but it assumed the GATE model over-simplifications were identical in all cases. It also allowed a superimposition with experimental data for HiRez which was purely cosmetic and did not change the ordering of the NEC curves in figure 2. That figure shows that when the axial length of the scanner is fixed, only the LSO 30 mm case provides higher NEC performance than the current HiRez. However this does not mean we should replace the 20 mm crystal by 30 mm ones, since for wholebody applications, increasing the axial FOV is a better strategy [8]. One should note in figure 2 that both $CeBr_3$ (30mm) and $LaBr_3$ (30 mm) NEC_{1R} curves are always below the LSO (20mm) curve. The curve crossing observed at 0.35 Ci/cc on the pixelated Anger-logic detector [2] also occurs on the HiRez but at a much higher activity concentration (around 1.3 Ci/cc) which is well beyond the clinical range. So the conclusion that $LaBr_3$ was a better choice than LSO above 0.35 Ci/cc [2] is only valid on the pixelated Anger-logic detector but not on the HiRez with its Pico electronics. In that particular comparison the higher density of LSO (see Table 1) is compensated by longer $LaBr_3$ (and $CeBr_3$) crystals, which also results in larger crystal

penetration or deterioration of the radial resolution when depth of interaction is not measured or not modeled in the reconstruction. Our conclusions are valid as long as TOF is not considered. Since $LaBr_3$ achieves a better timing resolution than LSO, the competition will likely be closer in TOF mode. Finally NEC performance is only a global aspect of the statistical quality of the data, quality of data corrections and image reconstruction method are other fundamental ingredients which will modulate the NEC locally.

V. CONCLUSIONS

With the HiRez geometry, its Pico electronics and the scintillators we considered, LSO appears to yield the best imaging performance as measured by peak NEC, due to the combination of high speed (fast decay time), high stopping power (high density and effective Z), and good energy resolution (good luminosity). The quest is not over yet: other crystals such as LuAP or LuI might be worth investigating, when commercially available, to try to outperform LSO.

VI. REFERENCES

[1] L. Eriksson, D. Townsend, M. Eriksson, M.E. Casey, M. Conti, B. Bendriem and R. Nutt, The NEC dependence of different scintillators for Positron Emission Tomography. NSS-MIC 2004 Conference Record, M10-8.

[2] Y. Bercier, M. Casey, J. Young, T. Wheelock and T. Gremillion, LSO PET/CT Pico performance improvements with ultra HiRez option, NSS-MIC 2004 Conference Record, M10-284.

[3] S. Surti, J.S. Karp. A count-rate model for PET scanners using pixelated Anger-logic detectors with different scintillators. Phys Med. Biol. 50(2005)5697-715

[4] S. Jan et al., GATE a simulation toolkit for PET and SPECT. Phys Med. Biol. 49(2004)4543-61

[5] Brun and Rademakers 1997 ROOT – An object oriented data analysis framework *Nucl. Instr. Meth.* A389 81-6

[6] A.L.Goertzen, J. Suk and C.J. Thompson, On the imaging of very weak sources in an LSO PET scanner. MIC 2006 Conference Record, M07-5

[7] M. Brambilla, C. Secco, M. Dominietto, R. Matheoud, G. Sacchetti, E. Inglese, Performance Characteristics Obtained for a New 3-Dimensional Lutetium Oxyorthosilicate–Based Whole-Body PET/CT Scanner with the National Electrical Manufacturers Association NU 2-2001 Standard, J. Nucl. Med., Vol. 46, 2005 , pp. 2083-91

[8] B.W. Jakoby, Y. Bercier, C.C. Watson, V. Rappoport, J. Young, B. Bendriem, D.W. Townsend, Physical Performance and Clinical Workflow of a new LSO HI-REZ PET/CT Scanner, MIC 2006, M14-186

Table I: NEC model parameters for all materials and crystal lengths considered.

Parameter	LSO-20	LSO-30	GSO-20	GSO-30	BGO-20	BGO-30	$LaBr_3$-20	$LaBr_3$-30	$CeBr_3$-20	$CeBr_3$-30
density [g/cc]	7.4	7.4	6.7	6.7	7.13	7.13	5.3	5.3	5.2	5.2
τ_{scint} [ns]	42	42	60	60	300	300	26	26	17	17
$n_{integration}$	3	3	3	3	1.3	1.3	2	2	2	2
τ_{reset} [ns]	10	10	10	10	10	10	10	10	10	10
τ [ns]	136	136	190	190	400	400	62	62	44	44
c_1	3.33	3.02	3.88	3.42	2.44	2.28	7.11	5.93	7.59	6.35
bkg	5668	8502	0	0	0	0	0	0	0	0
η_{si}	341751	404497	278747	346088	473438	538757	133256	182573	124887	170483
c_2	6.574	5.962	7.660	6.748	4.817	4.501	14.037	11.707	14.984	12.536
$\eta_{tr\_unscattered}$	572091	846178	383516	608051	739158	1027354	115106	233310	121128	213867
c_3	5.731	5.197	6.677	5.882	4.199	3.924	12.236	10.205	13.062	10.928
$\Delta\tau$ [ns]	4.5	4.5	8.	8.	10	10	4.5	4.5	4.5	4.5
n_{lor}	1589	1589	1589	1589	1589	1589	1589	1589	1589	1589
σ(E)/E	15%	15%	15%	15%	20%	20%	6%	6%	4%	4%
LLD [keV]	425	425	425	425	350	350	470	470	490	490
ULD[keV]	650	650	650	650	650	650	650	650	650	650
η_{si_rel}	1.00	1.18	0.82	1.01	1.39	1.58	0.39	0.53	0.37	0.50
η_{tr_rel}	1.00	1.48	0.67	1.06	1.29	1.80	0.20	0.41	0.21	0.37
Scatter Fraction	35.5%	35.6%	37.4%	35.6%	47.8%	45.6%	21.4%	20.2%	10.8%	11.4%